Journal of Structural Geology, Vol. 12, No. 1, pp. 1 to 17, 1990
Printed in Great Britain

0191-8141/90 $03.00 + 0.00

Palaeostress estimation using calcite twinning: experimental calibration and application to nature

K. J. ROWE and E. H. RUTTER*

Geology Department, Imperial College, University of London, London, SW7 2BP, U.K.

(*Received* 11 *November* 1988; *accepted in revised form* 8 *May* 1989)

Abstract—By means of high-temperature deformation experiments on calcite rocks of different grain sizes, we have established the relationships between differential stress and twinning incidence, twin density and volume fraction, and the way that these relationships depend on grain size. Both twinning incidence and volume fraction increase with grain size at a constant level of differential stress. Log twin density is proportional to stress but is independent of grain size. At a given grain size, volume fraction of twinning increases non-linearly with differential stress. Twinning activity measured by twinning incidence increases linearly with stress. The behaviour of each of these parameters is independent of temperature, strain and strain rate.

These relationships can be used as a basis for the estimation of palaeostress values in naturally deformed calcite rocks. This is illustrated by a study of twinning activity in limestones close to thrust faults in the Cantabrian zone of the Variscan orogenic belt in northwestern Spain. High peak differential stresses were measured, ranging from 150 to 250 MPa. Using the Turner Dynamic Analysis technique, however, it is clear that shear stresses resolved parallel to the fault planes were very low. The attainment of high stress differences when the resistance to faulting was low is attributed either to bending forces induced during the motion of the non-planar surfaces relative to each other or to the stress peak being attained prior to the localization of deformation onto the fault surfaces.

INTRODUCTION

SINCE the pioneering work of Turner (1953) it has been known that the incidence of twinning in calcite grains in marbles and limestones can be used to infer the orientation of the principal stresses which caused the deformation. Many successful studies of palaeostress orientations using the Turner Dynamic Analysis (TDA) technique have been reported (e.g. Turner 1953, Friedman & Conger 1964, Friedman & Stearns 1971, Spang 1972, 1974). Practical aspects of the use of the technique are reviewed by Turner & Weiss (1963) and Carter & Raleigh (1969).

More recently the possible use of twinning as an indicator of palaeostress magnitudes has been discussed (Jamison & Spang 1976, Friedman & Heard 1974, Tullis 1980, Spiers & Rutter 1984). From experimental studies, however, it is clear that twinning is easier in coarse-grained than in fine-grained rocks (Schmid & Paterson 1977, Casey *et al.* 1978, Spiers 1982, Spiers & Rutter 1984). This is because grain boundaries impede the spreading and widening of twin lamellae, which propagate through the crystal like a shear mode crack. Thus a practical palaeostress measurement technique must take grain size into account.

Spiers (1979, 1982) demonstrated that during deformation involving twinning, strain becomes heterogeneously distributed between grains, such that grains favourably oriented for twinning typically accommodate twice as much strain on the twinning systems as would be expected from the resolution of the bulk applied shear strain along the twin direction. He demonstrated that this leads to an approximately homogeneous distribution of *stress* between the grains. Although attempts have been made to measure bulk rock strains using twin lamellae (e.g. Groshong 1974), the strain inhomogeneity which typically develops must mean that strain estimates made from twinning overestimate the bulk rock strain due to twinning, but may underestimate any contribution from dislocation glide. The tendency for stress to be relatively homogeneous between grains in rocks deformed in the twinning regime is clearly of importance for the development of a useful palaeostress measurement technique.

The aim of this study has been to investigate the development of a practical palaeostress measurement technique based on calcite twinning, by means of an experimental rock deformation program which evaluates the effects of grain size, temperature, strain and strain rate on the twinning activity, and to seek to apply the technique evolved to a study of the stresses associated with the emplacement of some of the thrust sheets of the foreland fold and thrust belt of Variscan age in northern Spain (the Cantabrian zone).

EXPERIMENTAL METHODS AND MATERIALS

All experiments were carried out using fluid confining medium testing machines either of the type described by Rutter (1972) or Rutter *et al.* (1985). Constant strain rate compression experiments were carried out on oven-dry samples at confining pressures of 100–200 MPa, over strain rates ranging between 10^{-3} and 10^{-7} s^{-1}, at temperatures ranging from 200 to 800°C and to strains

*Present address: Department of Geology, University of Manchester, Manchester M13 9PL, U.K.

ranging up to 30% shortening. Raw mechanical data were corrected for the strength of the copper jacket surrounding the specimen, for axial apparatus distortion and for dimensional changes of the specimen (assuming constant volume deformation), so that true differential stress vs strain curves could be obtained.

Two different rock types (all >96% calcite) were employed for the experiments, a new block of Carrara marble and a coarse-grained marble from Taiwan. The porosities of these rocks are 0.2% and <1%, respectively. The mean grain sizes (determined using the linear intercept method on optical thin sections) are 150 and 400 μm, respectively, and neither of the rock types displayed a marked initial preferred crystallographic or grain-shape orientation. Prior to deformation, a few broad twin lamellae are typically found in Carrara marble. In the Taiwanese marble, however, most grains (but especially the larger ones) display a few thin twins, but these could easily be distinguished from the much broader, lenticular twins which were induced during high-temperature deformation (Fig. 1). Measurements were made only on the latter type of twin.

Unsuccessful attempts were made to locate a wider range of samples with different mean grain sizes, particularly in the range less than 150 μm. However, each of the above rock types displays a range of grain sizes, and it proved fruitful to divide the results of petrofabric studies into eight grain size class intervals for each rock type, thereby spanning the grain size range 50 μm–1.2 mm. For this operation, a representative diameter (d) of each grain was measured. This approach allowed overlap of grain size class intervals between different rock types, from which it could be shown that twinning behaviour in the same grain size intervals was consistent between the two rock types.

Twinning incidence (I_t) is defined as the percentage of grains in a given grain size class interval which contain optically visible twin lamellae. Petrographic studies of twinning incidence were made by Spiers (1982) on samples of Solnhofen limestone (grain size 5 μm) originally deformed by Rutter (1974). In the present study use will be made of these data, together with new measurements of twin density (No. of twins per mm) from these specimens, thus extending the grain size coverage down to 5 μm. In the new petrographic studies made on the Carrara and Taiwanese marbles, the percentage volume fraction (V) of twin lamellae in each grain was also measured, in addition to twinning incidence and twin density.

Measurement of the twinned volume of a grain can be carried out on a flat microscope stage provided care is taken to observe only the intersection of the top and bottom surfaces of each twin lamella with the plane of the thin section. Better results on flat surfaces can be obtained using polished thin sections which have been lightly etched with dilute hydrochloric acid (Fig. 2) imaged in a scanning electron microscope. Optical measurement of twinned volume was not possible in Solnhofen limestone, although it would be possible with the aid of scanning electron microscopy. In the two coarser rocks, the fraction of each grain occupied by each of one, two or three twin lamellae sets was measured by overlaying graph paper onto an image of each grain and assuming the areal fraction to be proportional to the volume fraction. No stereological corrections were applied to these data, which were stored on a computer database to facilitate interactive manipulation and graph plotting.

EXPERIMENTAL RESULTS OBTAINED

A summary of the new experiments performed is presented in Table 1. In all experiments, the rocks displayed fully ductile behaviour. Strain-hardening persisted up to about 400°C. At higher temperatures all rock types displayed steady-state flow after about 2% strain.

Typical I_t vs d, V vs d and number of twins per grain vs d data are presented in Fig. 3, together with histograms showing the relative numbers of grains examined in each class division (Fig. 4). For each deformed specimen the data shown are typically based on measurement of 200–300 grains. Because twinned volume is a function of grain orientation in each grain size class, range bars are shown in addition to the mean value. Twinned volume in the grains most favourably oriented for twinning is represented by the top of the range bar. It is not feasible here to show all of our experimental data in this form. The data presented are a representative selection.

Table 1 shows differential stress levels supported both at 10% total strain and at the maximum strain attained in each experiment. The latter is the stress level that pertains to the observed twin activity. For each rock type, the differential stress supported at 10% strain is shown as a function of strain rate and temperature (Fig. 5), allowing aspects of the rheological behaviour of the two marbles to be assessed and compared. Although rheological data for Solnhofen limestone and Carrara marble have previously been presented (Rutter 1974, Schmid *et al.* 1977, 1980), no previous studies of the Taiwanese marble have been published. It is beyond the scope of the present paper to explore the rheological contrasts between these various calcite rocks. However, it may be qualitatively noted that under the conditions of these experiments, in which flow is dominated by intracrystalline plasticity, strength increases with decreasing grain size, especially at the lower temperatures.

DISCUSSION OF EXPERIMENTAL DATA

Twinning incidence

Figure 6 shows that, for each of the three rock types, twinning incidence is largely independent of temperature and strain rate, but depends mainly on stress. The twinning incidence contours are displaced upwards, to higher stress levels, as grain size is reduced. Finite strains attained in the new experiments carried out for

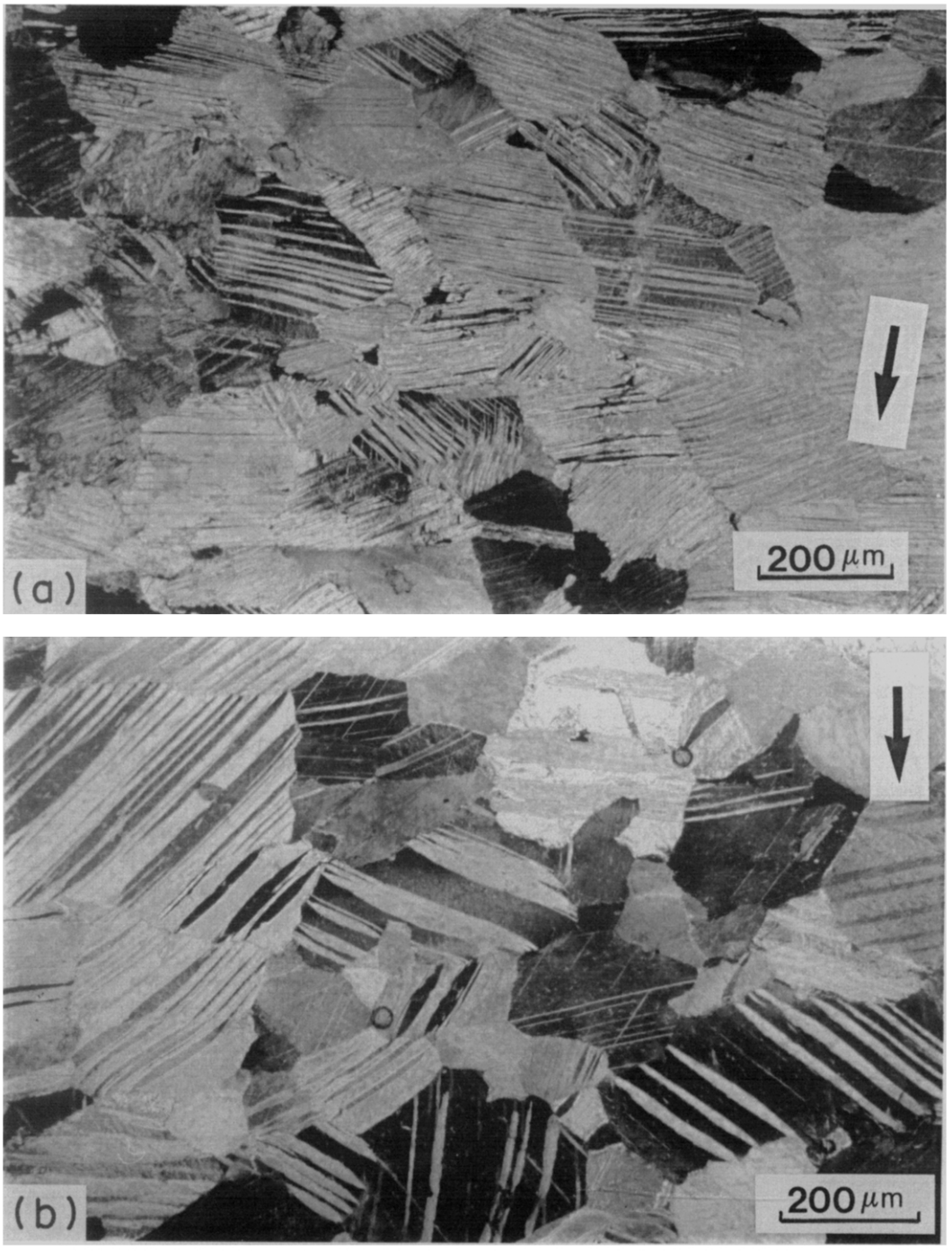

Fig. 1. Photomicrographs to show the contrasting morphology of (a) low-temperature (400°C, sample from block used by Rutter 1972) and higher temperature (600°C, block used for this study) twins in experimentally deformed Carrara marble. The low-temperature twins are many, thin and rational, whereas higher temperature twins are fewer and lenticular in shape, so that part of the twin boundary must be irrational. The compression direction is indicated by the arrow in each photograph.

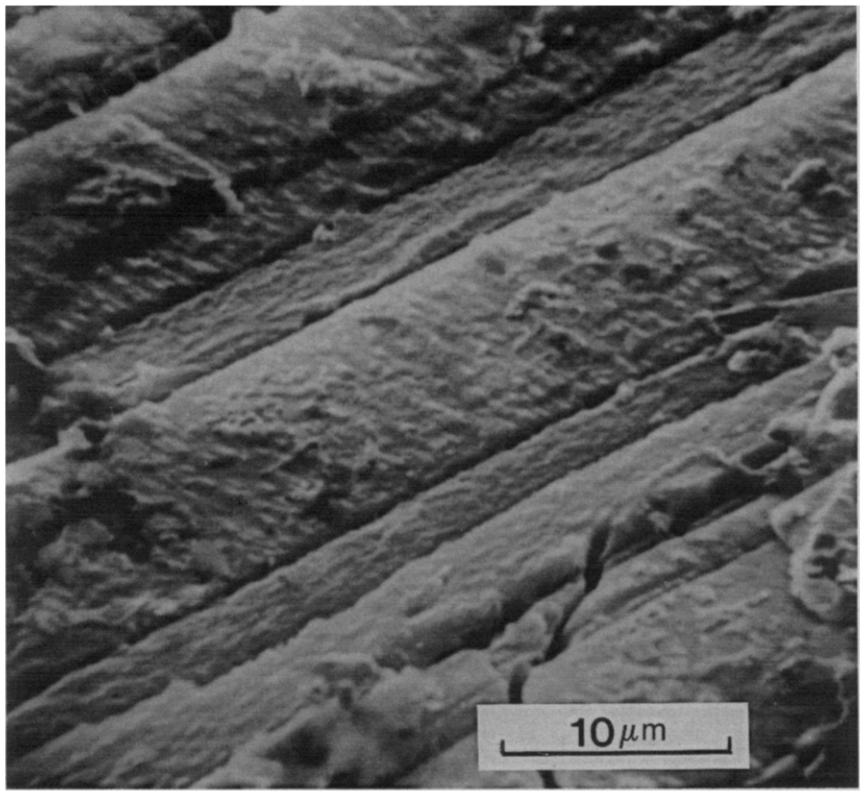

Fig. 2. Scanning secondary-electron micrograph showing the surface morphology of a partially twinned grain in Carrara marble experimentally deformed at 500°C. The surface has been lightly etched with dilute hydrochloric acid. Twin and host areas have etched at different rates, have contrasting surface features and the twin planes themselves have etched into narrow grooves. Volume % twinning can be estimated from such images.

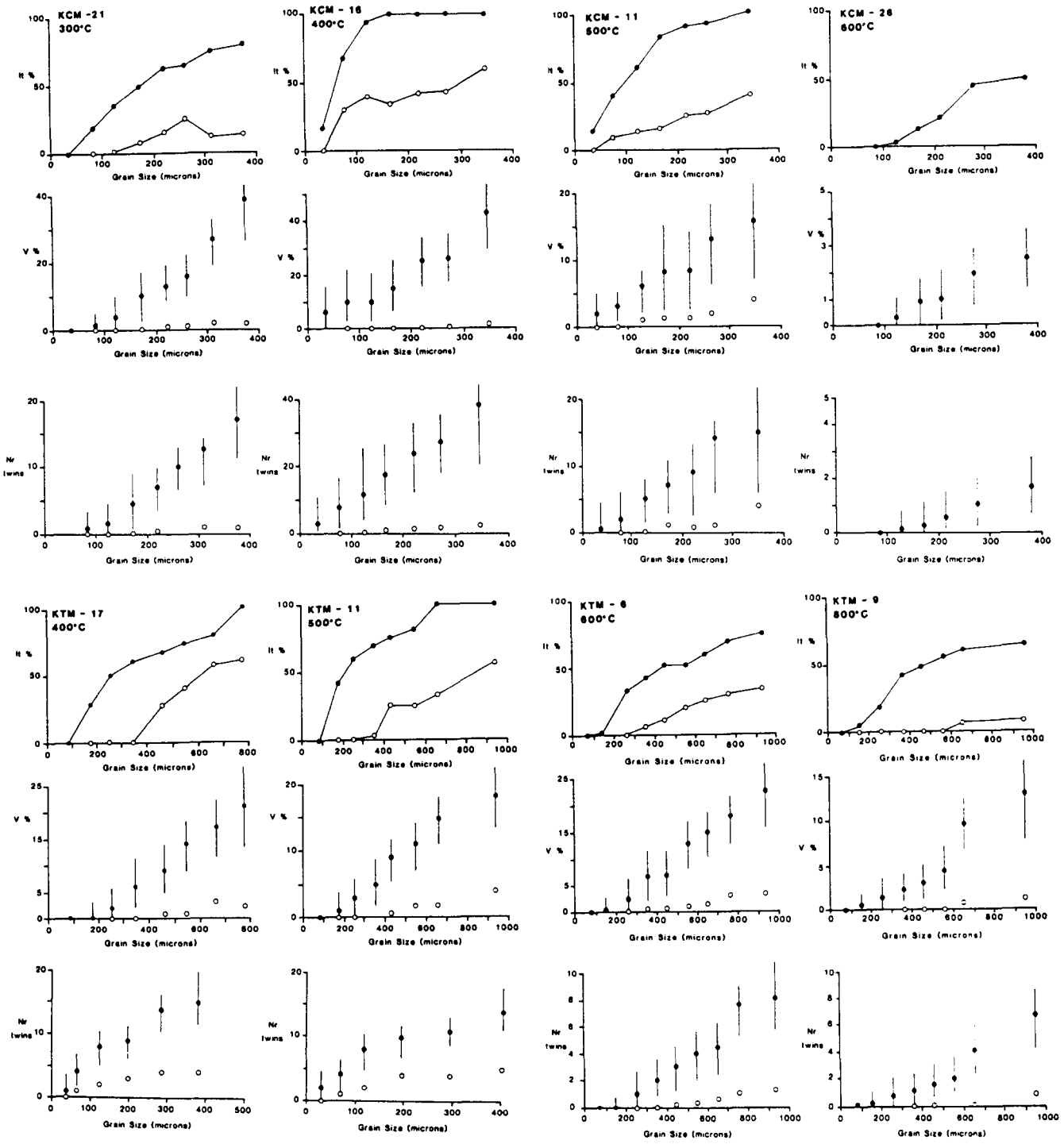

Fig. 3. Typical examples of data on twinning activity from experimentally deformed samples of Carrara marble (KCM series) and Taiwanese marble (KTM series). Experimental conditions for each run are given in Table 1. For each sample, twinning incidence (I_t), mean volume % twinning and No. of twins per grain are plotted against grain size class. Groups of measurements are shown on the plots for the principal twin set (black circles) and the secondary twin set (open circles). Range bars are shown on the V and No. of twin plots. The variation about the mean is due mainly to variations in the orientations of grains with respect to the applied stress directions. Typically, measurements on 200–300 grains were made for each deformed specimen.

this study ranged from 7 to 30% shortening. Figure 7 shows that V and I_t do not depend on strain in any systematic way. The lack of sensitivity of twinning activity to strain rate, temperature and strain is to be expected for a deformation process which is not thermally activated. This is an ideal characteristic of a palaeostress indicator. In fact, the Solnhofen limestone data suggest that twinning becomes *more* difficult at lower strain rates. Hence twinning palaeopiezometry may be expected to give somewhat conservative values for palaeostress. In this respect, our observations are in conflict with those of Jamison & Spang (1976) and Friedman & Heard (1974), who suggest that twinning is facilitated by high temperature and slow strain rates.

Figure 8 summarizes the I_t data for all rock types in the form of differential stress against log grain size for three

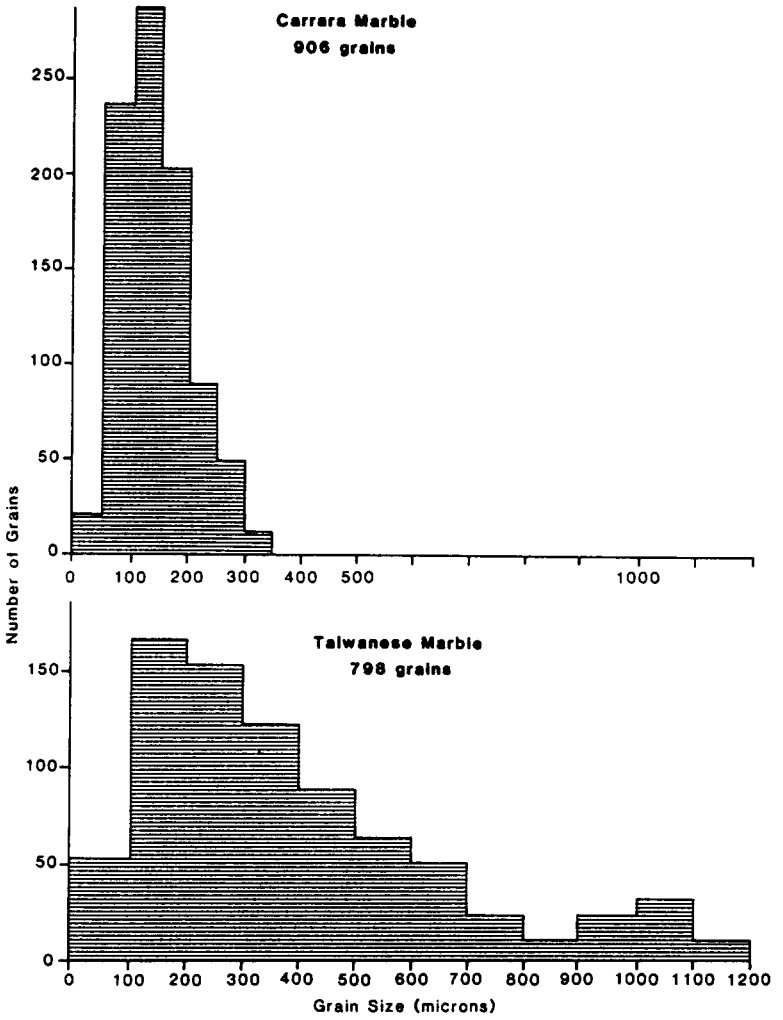

Fig. 4. Grain size distributions for the blocks of Carrara marble and Taiwanese marble used for the deformation experiments. The class divisions are the same as used in Fig. 3. The shape of the histograms shows the relative number of grains in each class division on Fig. 3.

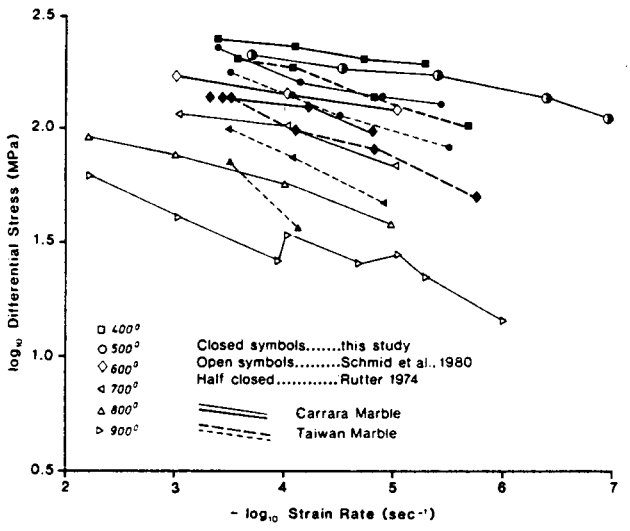

Fig. 5. Comparison of log differential stress at 10% strain as a function of −log strain rate for the samples deformed in the present study (closed symbols) with Carrara marble samples deformed by Schmid *et al.* (1980) (open symbols) and Rutter (1974) (half-closed symbols). The Carrara marble used in this study is slightly coarser (see Fig. 1) than that used by Rutter (1974), which may account for its lower strength at 500°C.

different I_t values, interpolated as required between pairs of points on the raw data graphs such as shown in Fig. 3. In this respect the behaviour of all three rock types is extremely consistent. In the experimental samples, I_t values rarely attain 100%, and this is a reflection of the fact that the samples have only been subjected to a simple, homogeneous stress field. However, in some large grain size classes I_t approaches 100% probably as a consequence of small sample sizes in the coarser classes. For a uniform crystallite orientation distribution, together with homogeneous stress and a large sample size of large grains, about 20% of the grains would be expected *not* to contain twins, owing to their unfavourable orientation (Spiers 1982).

The best-fit lines shown in Fig. 8 were obtained by multiple linear regression, and are described by the equation

$$\sigma = 523 + 2.13\, I_t - 204 \log d, \qquad (1)$$

where σ is the differential stress in MPa and d is the grain size in μm. The standard error on the estimation of stress was calculated to be 31 MPa. Also shown in Fig. 7 are the experimental data of Schmid & Paterson (1977) for the

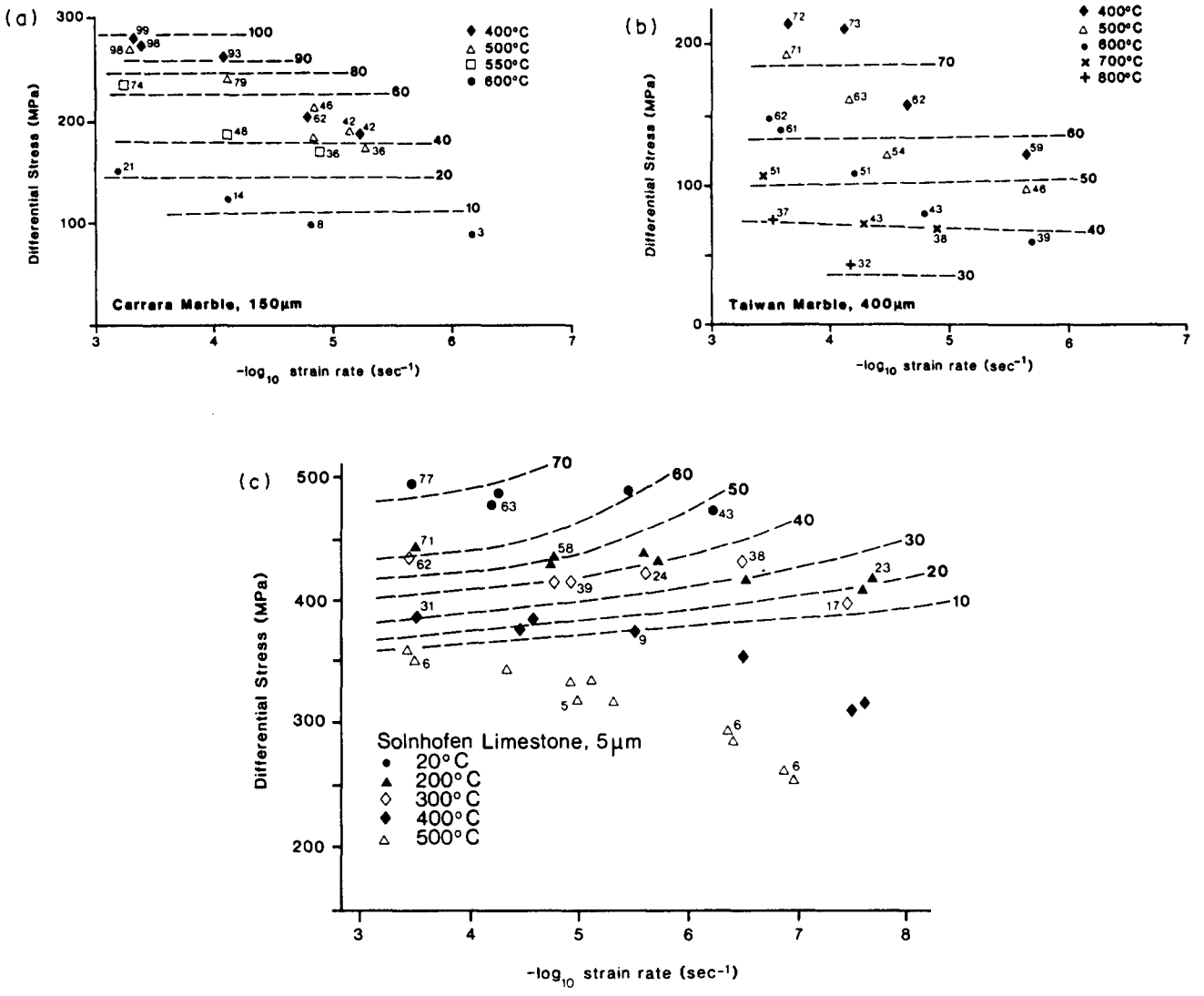

Fig. 6. Plots of differential stress supported at the end of each experimental run against −log strain rate for (a) Carrara marble, (b) Taiwan marble and (c) Solnhofen limestone. The figure beside each plotted point is the I_t value at the grain size indicated. The Solnhofen limestone data were derived from the experiments of Rutter (1974) by Spiers (1982). In each figure contours of constant I_t are shown. I_t is largely independent of temperature and strain rate, and depends mainly on stress. At high stresses in Solnhofen limestone, however, twinning becomes more difficult with decreasing strain rate.

estimated stress–log grain size relation for the onset of twinning in Solnhofen limestone, Carrara marble and an oolitic limestone of variable grain size. Their data are clearly consistent with ours at the level of <10% twinning incidence.

If equation (1) is to be used for palaeostress measurements on naturally deformed rocks, reasonable results will be obtained only from samples loaded in a single, coaxial, strain-inducing event, otherwise stress levels will be overestimated. This is because twinning will be activated in grains in a wider range of orientations than would otherwise be the case. In this respect, our I_t data simply represent a basis for a refinement of the method of palaeostress estimation outlined by Jamison & Spang (1976), taking into account grain size effects (which they were unable to do), and is subject to the same limitations. In principle, the complexity of the loading history can be investigated using the TDA technique. If a simple loading picture emerges from this, the measurement of I_t and grain size represents a very rapid means of estimating palaeostress magnitudes.

Twin density

Twin density (D) is here defined as the rate of change of the number of lamellae of a given twin set with respect to grain diameter measured normal to the trace of the twin lamellae. Figure 3 shows that this parameter, equal to the slope of the graphs (least-squares best-fits on the mean values shown) of number of twins per grain against grain size, is fairly constant for a given specimen. Hence the No. of twins per mm is a constant which is *independent of grain size*. However, the twin density (D) increases with differential stress. Figure 9 shows that a reasonably linear variation of stress with log twin density exists, given by

$$\sigma = -52.0 + 171.1 \log D \qquad (2)$$

with a standard error of 43 MPa on the best-fit line. The behaviour appears to be consistent between the three rock types studied, hence this relationship may be used as a basis for estimating palaeostress levels in naturally deformed rocks. It is relatively easy to ascertain whether

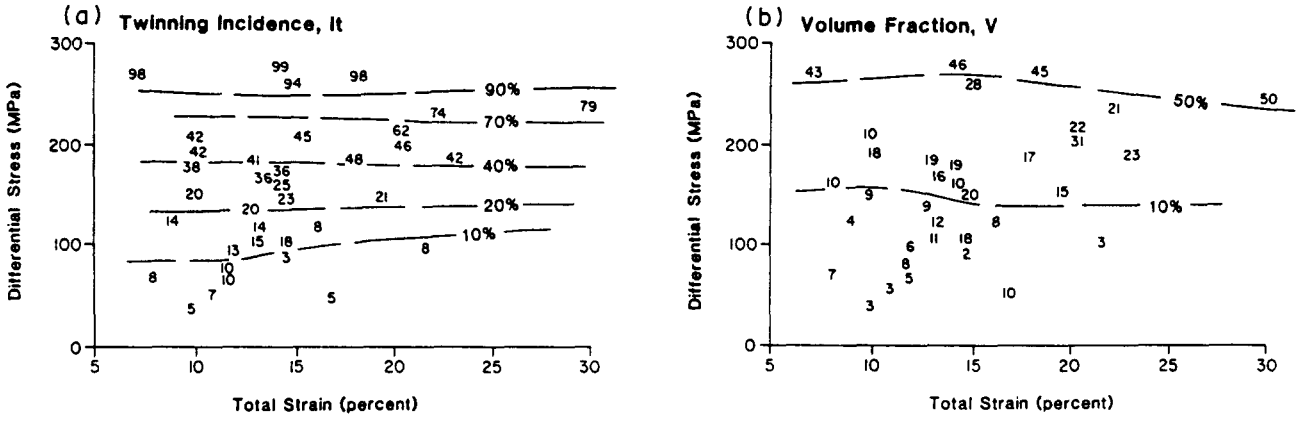

Fig. 7. Plots of differential stress against total strain attained for the experiments on Carrara marble and Taiwan marble. In (a) data points are shown at I_t values at 150 μm grain size. In (b) data points are shown as V_{max} values at 300 μm grain size. In each case the contours sketched show that these measures of twinning activity depend on stress but are independent of strain.

a naturally deformed rock displays a graph of number of twins vs grain size of constant slope.

The relative constancy of twin density in each experimental specimen may mean that at a given stress level the density of nuclei for twin formation is fairly constant around all grain boundaries. The scatter of points may be a reflection of the intrinsic variability of this density. The standard error is equivalent to the statement that the density of nuclei varies by ±50% about the mean value at constant stress. Compared to the twinning incidence method, it is to be expected that palaeostress measurements using twin density should be less sensitive

Table 1. Summary of experimental data. KCM samples are Carrara marble, KTM series are Taiwanese marble. I_t values are given for the mean grain size of the rock, 150 and 400 μm for Carrara and Taiwanese marbles, respectively. V_{max} values are given only for three grain size intervals, but analysis was based on eight intervals. Twins/mm is the slope of the graph of No. of twins per grain vs grain size

Sample No.	Temp (°C)	Confining pressure (MPa)	Strain rate (s^{-1})	Max strain (%)	Stress at		Max volume % at grain size (μm)			I_t (%)	Twins/mm
					Max strain	10% strain	100	300	800		
KCM10	500	106	4.4E-4	18.3	270	240	15	45	—	98	82
KCM11	500	104	8.3E-5	30.1	243	163	6.4	19	—	79	50
KCM12	500	104	1.8E-5	13.2	183	140	6.4	18.5	—	41	47.5
KCM14	500	105	4.5E-6	14.2	175	133	6	18.5	—	36	37.5
KCM19	400	140	1.8E-5	20.3	214	204	8	22	—	62	37.2
KCM20	400	140	5.0E-6	10.1	190	188	6.1	18	—	42	18.6
KCM13	550	106	4.7E-4	22.1	234	180	7	21	—	74	33
KCM15	550	104	8.5E-5	18.0	185	160	5.6	17	—	48	33
KCM27	550	103	1.2E-5	13.4	170	157	5.3	16	—	36	18.3
KCM16	400	102	4.2E-4	14.4	280	252	16	46	—	99	108.3
KCM17	400	104	8.4E-5	15.0	263	230	9.6	28	—	94	80
KCM18	400	104	3.7E-4	7.1	273	252	13	43	—	98	68
KCM21	300	170	2.3E-5	20.4	203	177	8	30.5	—	46	52.5
KCM22	300	171	5.6E-6	23.1	191	160	5	23	—	42	65
KCM23	200	203	5.7E-7	14.8	91	—	0.2	1.7	—	3	3
KCM24	600	105	5.8E-4	19.5	152	136	4	14.5	—	21	12.5
KCM25	600	104	8.0E-5	9.1	126	125	1.4	4.2	—	14	3.5
KCM26	600	104	2.0E-5	21.8	100	102	0.8	2.8	—	8	6.3
KTM1	700	104	3.5E-4	14.7	106	100	6	18	50	51	24
KTM2	700	104	5.9E-5	7.9	72	72	2	6.5	18	43	5
KTM3	700	104	1.8E-5	16.8	52	52	0	10	35	38	11
KTM4	600	104	3.0E-4	14.8	149	142	7	20	54	63	28
KTM5	600	104	6.0E-5	13.1	108	102	3	10.5	27.5	51	16.4
KTM6	600	105	1.6E-5	11.6	80	85	1	8	24	43	10.2
KTM7	600	103	2.5E-6	10.9	59	55	1	3.2	9	40	8
KTM15	600	104	2.8E-4	12.8	140	140	3	8.5	23	61	9.8
KTM8	800	103	6.6E-5	9.8	42	39	0.5	3.1	9	32	5
KTM9	800	103	3.4E-4	11.5	74	70	1.5	5.3	14	37	7.6
KTM14	500	103	3.0E-6	11.9	97	92	2	6	16.5	46	7
KTM18	400	107	2.8E-6	16.2	122	113	0	7.5	20.9	59	9.3
KTM10	500	104	6.8E-5	14.2	161	150	3	9.5	25	63	27.7
KTM11	500	104	3.1E-4	9.8	191	188	2.4	7.5	21	71	14.1
KTM12	500	104	3.4E-5	13.1	120	116	4	12	34	54	23
KTM13	400	105	2.8E-4	9.8	214	214	3.3	9.5	25	72	10.4
KTM16	400	104	7.0E-5	15.2	209	203	4	12	30	73	10.8
KTM17	400	105	1.1E-5	9.8	156	156	0	8.5	29	62	10

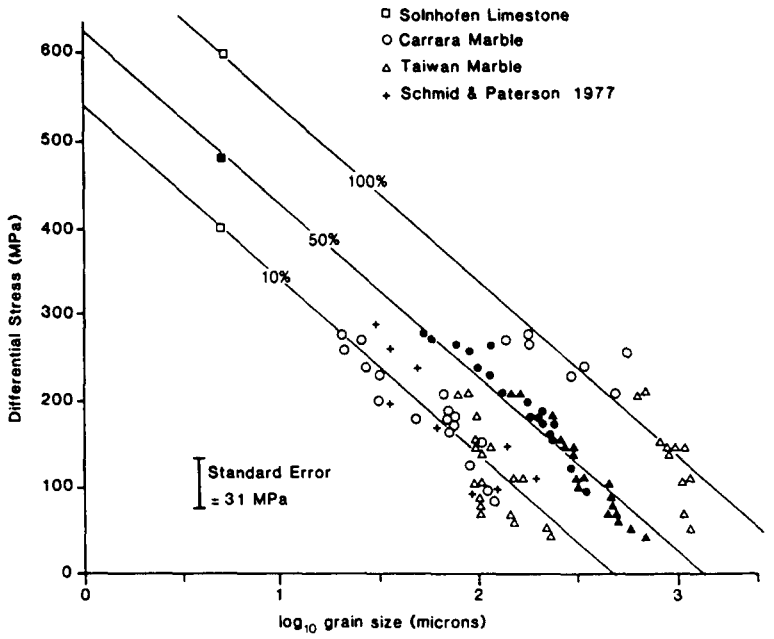

Fig. 8. Plot of differential stress against log grain size for constant values of I_t of 10, 50 and 100%, derived from I_t data of the type shown in Fig. 3. The grain sizes shown for Carrara and Taiwan marbles correspond to the centres of the class divisions from which measurements were taken, whilst the Solnhofen limestone grain size is the mean size and all grains are included in the sample. The I_t = 50% data are distinguished from the other I_t data by the use of filled symbols. The best-fit lines shown were obtained by multiple linear regression. Also shown for comparison are the estimates of grain size and stress for the onset of twinning as made by Schmid & Paterson (1977) for Solnhofen limestone, Carrara marble and the variable grain size matrix of an oolitic limestone.

to the complexity of the deformation history, provided that the number of twin nuclei around a given grain boundary is not significantly affected by variations in principal stress orientations.

No systematic effects of temperature could be detected in the behaviour of σ vs D. The stress required to activate twinning is likely to vary with the shear modulus, which decreases with temperature. This effect is, however, expected to be small compared to the scatter of points about the best-fit line.

Volume % twinning

Schmid factor, m, is defined as $\cos\phi \cos\psi$, in which ϕ is the angle between the maximum compression direction and the normal to a twin plane of a single grain, and ψ is the angle between the compression direction and the twinning displacement vector. Resolved shear stress along the twinning vector is maximized when ϕ and ψ are each 45°. Hence m varies between 0 and 0.5, according to the grain orientation. Spiers (1979) showed that

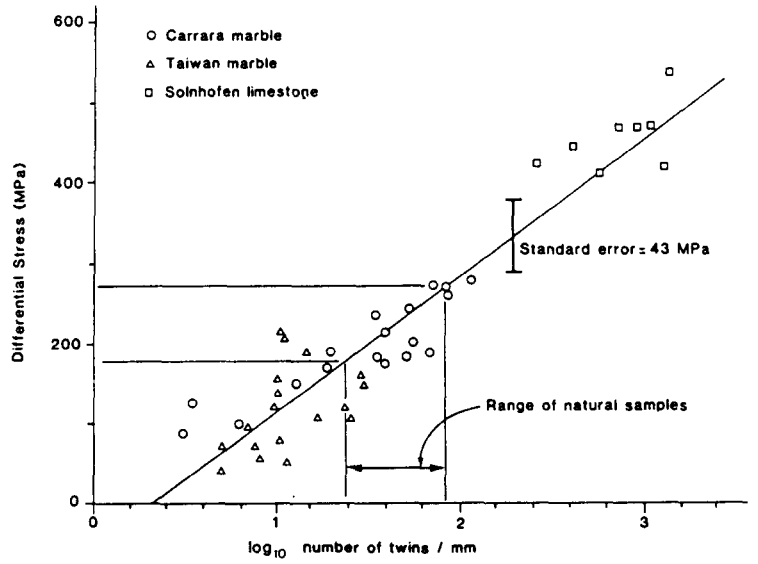

Fig. 9. Plot of differential stress against log No. of twins per mm (each point represents the slope of the best-fit line on the plots of mean values of number of twins per grain vs grain size as shown in Fig. 3). The best-fit straight line shown is $\sigma = -52.0 + 171.1 \log D$, where D is the No. of twins per mm. The range of twin densities observed in the natural samples studied (see Table 2) is indicated, together with the corresponding range of inferred stress values.

for calcite, volume % twinning in a single deformed sample is linearly proportional to the Schmid factor (Fig. 10).

Data of the type shown in Fig. 3 demonstrate that for deformation to a given stress level, volume % twinning is approximately linearly proportional to grain size, for each twin set observed. When combined with the above observations of constant twin density irrespective of grain size, it is clear that in order to account for the V behaviour, the average thickness of twins must increase linearly with grain size.

The range bars shown for each grain size reflect variations of orientation of grains, the maximum on the range bar (V_{max}) corresponding to the grain or group of grains for which m is greatest. Thus, unlike the I_t parameter, the maximum twinned volume in a particular grain size class measures the maximum stress applied, *irrespective* of the complexity of the deformation history or of variability of orientation of the applied stresses.

The relationship observed between V_{max} and grain size for a given sample suggests that there may be no minimum grain size below which twinning does not develop. Rather, at low stresses in small grains, twinning activity may be so low that it may fail to be detected, especially in unfavourably oriented grains. The twinning incidence data, on the other hand, suggest that there may in fact be a minimum grain size for twinning at a particular stress level. Lack of grain size resolution below 100 μm precludes a clear answer to this question at this time.

In order to develop a practical palaeopiezometer based on V_{max}, in Fig. 11 we plot differential stress vs V_{max} for different grain sizes. The points are extracted from best-fit straight lines to V_{max} vs grain size for each experiment, from both tested rock types. The V_{max} values given in Table 1 are sufficient to define the V_{max} vs grain size straight line for each experimentally deformed sample. Graphical manipulation of the data suggested that it should be best described by a relation of the form

$$\log \sigma = \log A + m \log d - n \log V \qquad (3)$$

in which, owing to the linear relation initially assumed between V and d, it is expected that $m = -n$. Multiple linear regression on the raw data yielded

$$\log \sigma = 2.90 - 0.47 \log d + 0.40 \log V. \qquad (4)$$

Refitting the data about the same centroid with the constraint that $m = -n$ gives

$$\log \sigma = 2.72 + 0.40 (\log V - \log d). \qquad (5)$$

In Fig. 11 data for grain sizes of 100, 400 and 1000 μm are shown, together with curves of functions 4 and 5, transposed on to a linear plot of stress vs grain size.

From measurements of V_{max} at different grain size intervals for a naturally deformed rock the maximum applied stress difference can be estimated. The figure obtained would be independent of the complexity of the stress history, provided that there is no intense crystallographic preferred orientation in the rock which might lead to the maximum possible V not being developed.

The scatter of the points shown for the three grain sizes in Fig. 11 is typical of the data for other grain sizes, and is a reflection of the following sources of uncertainty:

(a) the grain orientation which would yield V_{max} is not always available in the sample of the particular grain size interval;

(b) the grain size intervals are discrete and arbitarily chosen;

(c) stress heterogeneities (magnitude and orientation) exist from grain to grain (from the work of Spiers 1979, the orientation heterogeneity can be expected to be about 15°);

(d) uncertainty exists in measured differential stress in experiments, arising from errors of measurement and strain heterogeneity (specimen barrelling). This source of error is of the order of 1–10%;

(e) errors in the measurement of V may typically be of

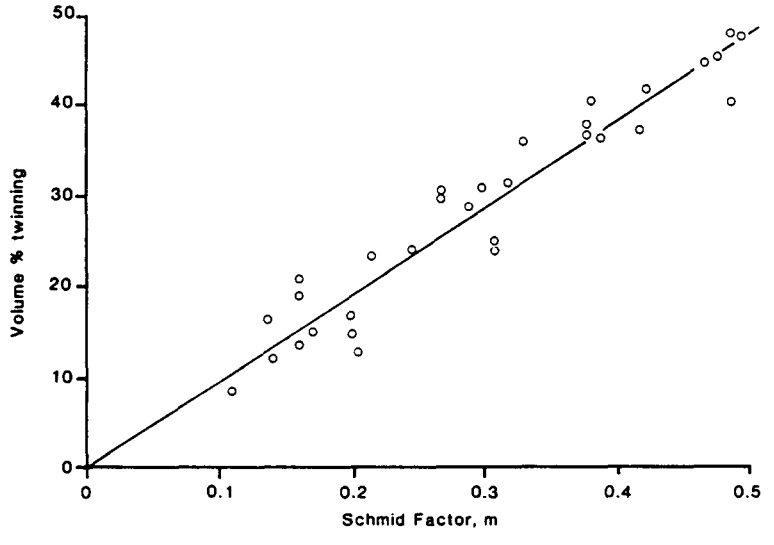

Fig. 10. Data of Spiers (1979) which show the linear proportionality between Schmid factor, m, and volume % twinning in an experimentally deformed, coarse-grained marble.

the order of 10–20%, depending on grain size. The larger errors may arise for the more irregularly shaped twins formed at high temperatures;

(f) grain size is estimated as a diameter measured on a two-dimensional surface. This is always smaller than the true grain diameter. If it is very much smaller then V may appear larger than would be expected for the apparent grain size. If the spacing between twins and the twin thickness is non-uniform, an additional non-systematic error in V also arises from this effect;

(g) a further possible source of error arises from the fact that in order to obtain a range of twinning activities at low stress levels we have had to carry out some experiments at quite high temperatures (600–800°C). Higher temperature twins in calcite differ in morphology from low-temperature twins. They are typically lensoid in shape and have irrational boundaries, especially near grain boundaries. In contrast, low-temperature twins are typically thinner and are bounded by rational planes along a greater proportion of their length (Fig. 1). The same V at low temperature appears to be accomplished by a greater number of thinner twins than at high temperature (Fig. 1). This may mean that some twinned volume at high temperature arises by diffusion-accommodated twin boundary migration, and may account for the greater amount of scatter of data at low stress levels seen on Fig. 11.

The cumulative effect of these sources of error is seen as the vertical (stress) range of data points on either side of the fitted curves in Fig. 11. The standard error of a stress estimate using these curves was calculated to be 41 MPa at any stress level. This level of uncertainty can be verified by back-estimating the flow stresses for the experiments using the V_{max} data together with the set of best-fit curves. Bearing in mind the very systematic relationship observed between V and grain size in individual experimental samples, it is clear that most of the scatter in Fig. 10 arises from differences in twinning behaviour *between* individual rock samples deformed at different stresses. In the light of the results obtained to date, further experimental and petrofabric studies would be required to establish whether it will be possible to reduce the level of uncertainty in palaeostress measurements using these techniques.

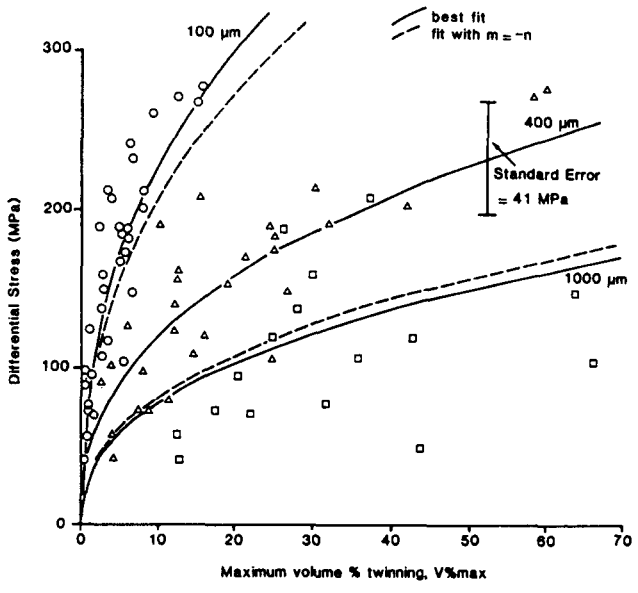

Fig. 11. Data extracted from the graphs of volume % twinning against grain size as shown in Fig. 3, showing the relationship between applied differential stress and *maximum* volume % twinning, for grain sizes of 100, 400 and 1000 μm (circles, filled triangles and squares, respectively). The data were fitted to the function $\log \sigma = \log A + m \log d + n \log V$ by multiple linear regression. For the continuous curves, $\log A = 2.90$, $m = -0.47$ and $n = 0.40$. For the dashed curves, $\log A = 2.72$, $m = -n = -0.40$, with the same centroid as for the continuous curves. For clarity, data for grain sizes of 200, 300, 500, 600 and 800 μm, also used for the regression analyses, are omitted from the figure.

APPLICATION TO NATURALLY DEFORMED ROCKS

We now apply the experimental results to twin activity in limestone samples from the Cantabrian zone of northern Spain. This is a foreland fold and thrust belt of strongly arcuate trend. A review of the regional geology is presented with a new tectonic synthesis of the belt by Pérez-Estaun *et al.* (1988).

Samples collected and results obtained

Two localities were sampled:

(a) from two imbricate slices in the hangingwall of the Somiedo Nappe, respectively named here as the Santa Lucía and Portilla tectonic wedges (because the limestones of the Santa Lucía and Portilla Formations, respectively, are cut by the thrust planes). Oriented samples were collected from limestones of the same lithological type in both hangingwall and footwall, where the two thrusts crop out 450 m to the north-west of the village of Torrestio and 200 m to the east of the village of La Cueta, respectively. In these wedges the rocks have suffered relatively simple deformation histories, involving thrust displacements of only tens of metres;

(b) samples were collected from the footwall of the Esla Nappe. This nappe is one of the highest and oldest in the thrust belt. All of the samples were collected from the Portilla Limestone Formation, which forms the footwall flat, at varying distances (from 0 to 12 m) from the thrust plane, where it crops out 300 m east of the village of Corniero. The displacement on the overthrust at this point is about 19 km (Alonso 1987). The hangingwall flat unit (Láncara Limestone Formation) is very fine grained and dolomitic, and not suitable for twinning studies. The footwall is likely to have suffered a less complex deformation history, although it has still been warped as a result of transport upon the underlying Corniero Nappe.

I_t, No. of twins and V data as a function of grain size class are shown in Fig. 12 for a representative selection of the samples collected; relevant numerical data are listed in Table 2. The form of these data should be compared to the corresponding plots for the experimentally deformed samples (Fig. 3). In all respects the

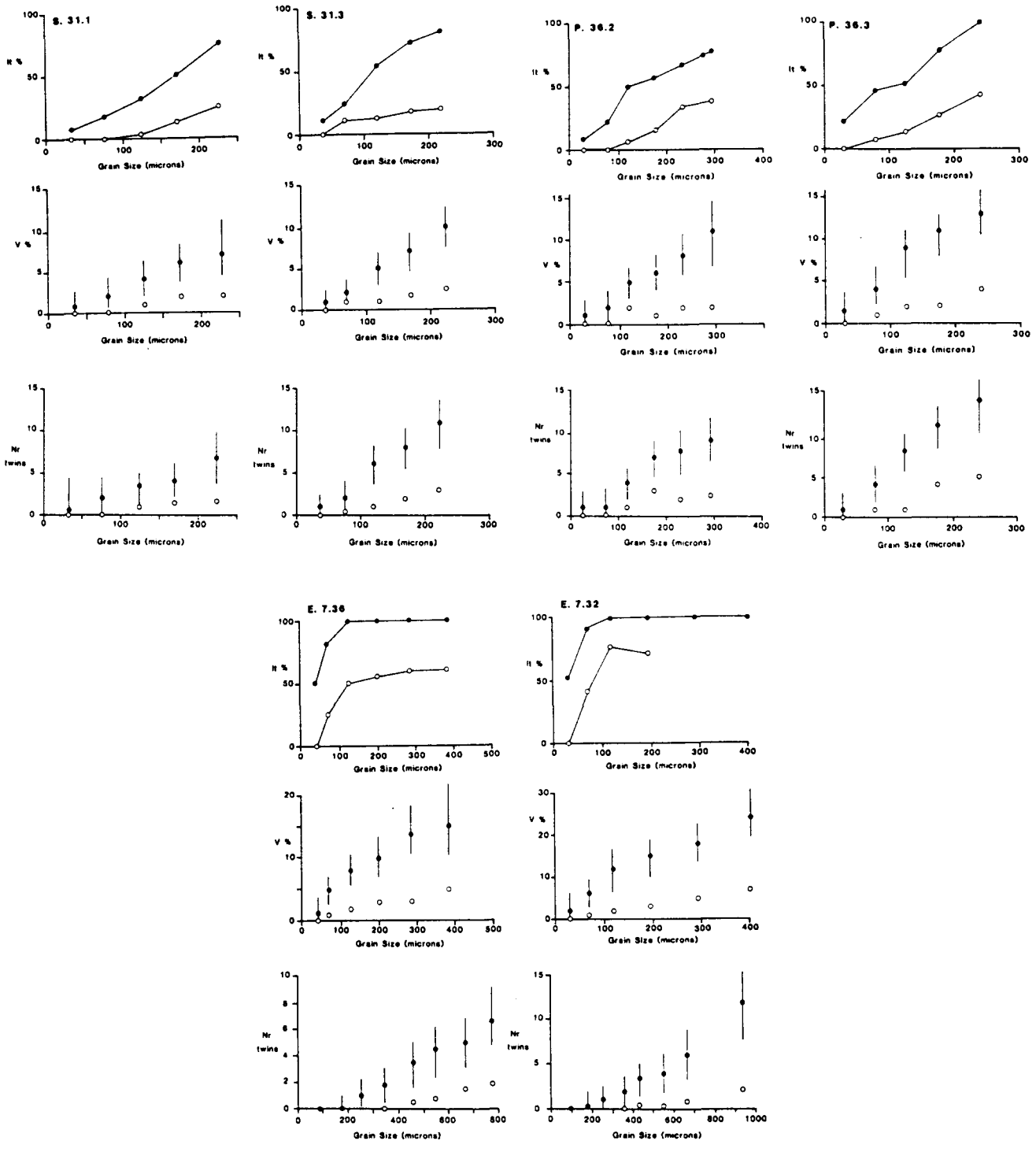

Fig. 12. Typical results of microstructural studies of twinning activity in naturally deformed limestones from the Cantabrian fold and thrust belt of northern Spain. The data are presented in the same way as the experimental results shown in Fig. 3. Samples prefixed S and P are from the Santa Lucía and Portilla tectonic slices in the hangingwall of the Somiedo Nappe. Samples prefixed E are from the footwall of the Esla Nappe.

patterns of twin behaviour of the naturally deformed rocks are closely comparable to the experimentally deformed samples, despite large differences in temperature and strain rate.

Figure 13 illustrates how the V_{max} values for different grain size classes measured for the naturally deformed rocks are used, together with the best-fit curves to the experimental data, to infer differential stress. The tendency for smaller grain sizes to estimate higher stresses is typical of the naturally deformed samples (especially those from the Esla Nappe) relative to the experimentally deformed material. It is thought to be a consequence of the greater microstructural complexity of the natural materials and to the more complex stress history they have suffered. The lower stress value, characteristic of a wider range of grain sizes, has been taken as the more representative one.

Figures 14 and 15 show the stress levels which can be

Table 2. Measurements of twinning incidence (I_t), maximum volume percent twinning (volume %) and twin density (twins/mm) made on naturally deformed limestones, and the differential stress values estimated from them. Distances from the fault plane are given in metres as negative in the footwall, positive in the hangingwall. Samples prefixed E are from the Esla Nappe, S from the Santa Lucía tectonic wedge (Somiedo Nappe) and P from the Portilla tectonic wedge (Somiedo Nappe)

Sample No.	Distance from fault (m)	Grain size at I_t			Estimated stress (MPa)	Volume % at grain size (μm)				Estimated stress (MPa)	Twins/mm	Estimated stress (MPa)
		10%	50%	100%		100	200	300	500			
E.7.28	−0.2	<100	<100	<100	>400	17.5	26.5	34	—	210	52.3	242
E.7.29	−0.25	<100	<100	<100	>400	14.6	21.6	28	—	200	52	240
E.7.30	−0.5	<100	<100	<100	>400	18	26	35	44	220	78.7	275
E.7.31	−0.95	<100	<100	<100	>400	14	21.3	29	—	210	43.3	229
E.7.32	−2.7	<100	<100	400	>400	11.4	18.2	24.6	31.5	190	28.3	200
E.7.33	−12.0	<100	<100	400	>400	9.2	15.8	23	28.5	185	28.8	202
E.7.34	−2.0	<100	<100	400	>400	17.6	30	42.5	55	236	75	270
E.7.35	−4.8	<100	<100	400	>400	11.2	17	23	29	185	32	210
E.7.36	−8.8	<100	<100	400	>400	7.2	13	18.6	—	175	38.4	218
S.31.1	−1.9	55	170	310	230	5.4	10	—	—	170	32	210
S.31.2	−0.75	60	220	420	200	4	8.2	13.2	—	150	37	215
S.31.3	−0.2	25	120	250	350	5.5	11	16	—	165	56	250
S.31.4	+2.0	3	205	450	200	5	8.5	12.2	—	145	32.3	211
S.31.5	+0.7	0	110	270	250	6.5	13.6	18.6	—	175	48	239
S.31.6	+0.1	0	70	230	270	11.8	20	—	—	210	64.4	270
P.36.1	−2.0	60	210	420	200	3.2	6.2	9.7	12.9	135	23	180
P.36.2	−0.9	15	170	360	210	5.5	10	14.8	—	160	35	215
P.36.3	−0.25	0	110	250	240	7.5	14.1	22.5	—	185	62.5	260
P.36.4	+1.0	0	125	320	230	7	12	—	—	165	44	230
P.36.5	+0.4	0	105	300	240	9	15.6	—	—	190	53.3	245

inferred from I_t, D and V_{max}, respectively. In the case of the Somiedo Nappe samples, the I_t and D methods estimate significantly higher differential stresses than the V_{max} method. For the Esla Nappe samples, every grain shows at least one twin set in all grain size intervals, implying that the stress history has been complex and making it impossible to obtain stress estimates using the I_t method. The D method allows stresses to be estimated, however, and these are all systematically higher than those obtained using the V_{max} method (Fig. 15).

For the Somiedo Nappe samples, all three methods of estimation suggest that the stress increases slightly towards the thrust plane on both the hangingwall and footwall sides (Fig. 14). Figure 15 shows a slight decrease in stress with distance from the Esla Thrust in its footwall. These results suggest that a much wider areal coverage is required in order to detect substantial variations in the peak stresses recorded.

A more complete interpretation of these data requires a Turner Dynamic Analysis (TDA) in order to reveal the

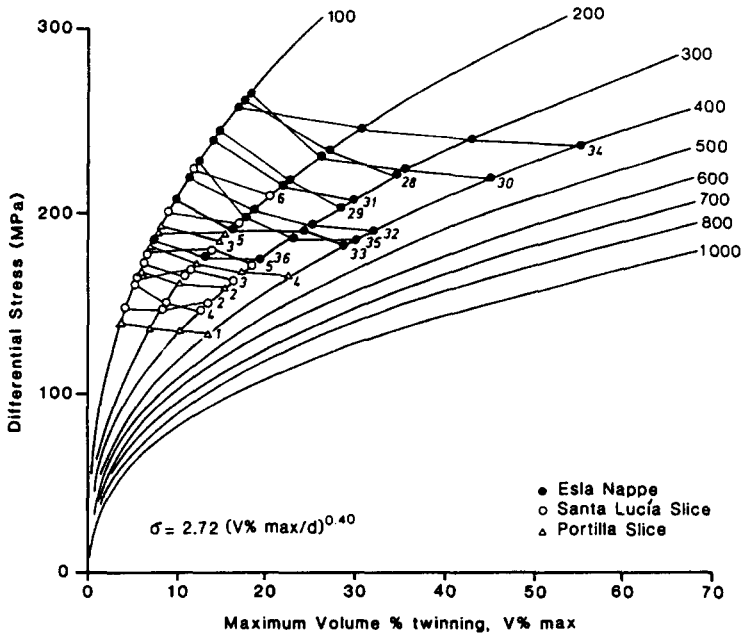

Fig. 13. Plot of equation (4) (inset bottom left) showing differential stress against maximum volume % twinning for constant values of grain size (μm) and its use to estimate palaeostress values for naturally deformed limestones from the Cantabrian zone of northern Spain. Measurements of maximum volume % twinning from individual specimens are identified by the numbers shown. These correspond to the specimen numbers listed in Table 2.

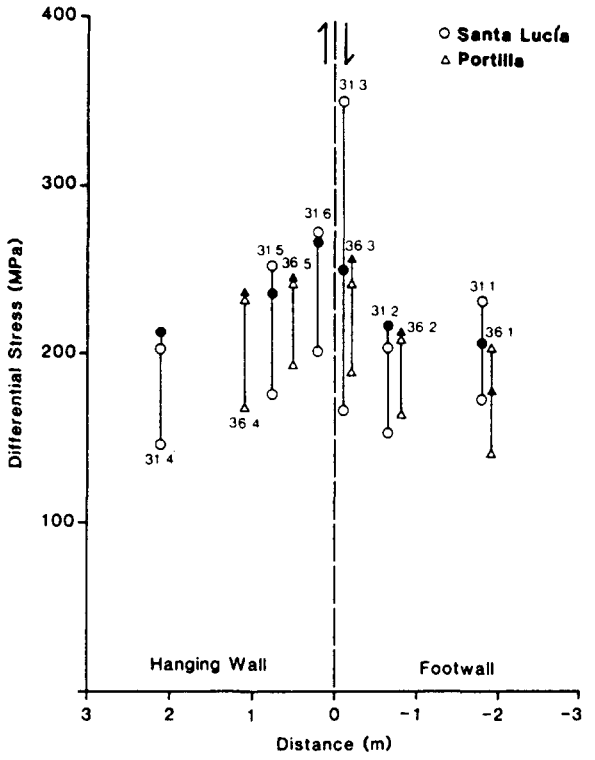

Fig. 14. Values of differential stress inferred using both the I_t (open symbols, higher values), V_{max} (open symbols, lower values) and twin density (closed symbols) methods for the Santa Lucía and Portilla tectonic slices of the hangingwall of the Somiedo Nappe. The stress values (listed in Table 2) are shown as a function of distance above and below the thrust planes.

orientation of the principal stresses. These results for the Esla and Somiedo Nappe samples are shown in Fig. 16.

The Somiedo Nappe results show a tendency at both localities for σ_1 axes to be concentrated in the thrust transport direction (inferred from the geometry of the units as mapped in the field) in *both* the hangingwall and footwall. The σ_3 axes also tend to lie in the thrust plane, normal to the transport direction. These broad features are regarded as significant because concentrations up to several times uniform are recorded, but the subsidiary concentrations within the broad maxima are probably sampling artifacts.

Despite a larger sample size, the Esla Nappe samples show much more complex behaviour, with both σ_1 and σ_3 axes widely scattered and only low concentrations being produced (locally up to three times uniform, which may only be through sampling fluctuations). There appears to be a weak tendency for both σ_1 and σ_3 axes to lie in a great circle girdle normal to the thrust plane and intersecting it in the transport direction (as inferred from the regional geometry of the stacking of the overthrust sheets). A concentration of σ_3 axes is also developed on the thrust plane at 90° to the transport direction. This broad spread of the inferred palaeostress principal axes explains the fact that all grains are twinned in these samples.

Interpretation and discussion

Considering first the Somiedo Nappe results, the parallelism of the maximum principal stress (σ_1) directions with the thrust transport direction, as indicated by the TDA, must mean that shear stresses resolved along the thrust plane were always very low. From geological cross-sections (Pérez-Estaun *et al.* 1988) the overburden pressure at the time that these faults were active might have been as much as 200 MPa. If the fault planes were flat-lying at the time of slippage and the pore pressure corresponded to a hydrostatic head of water, then, on the basis of laboratory-determined friction coefficients, shear stresses resolved along the faults would be expected to be of the order of 110 MPa (differential stresses of *ca* 280 MPa, only slightly higher than that observed) but the maximum principal stress would lie at about 30° to the fault plane. Thus the fault rocks may have had an intrinsically low shear strength, coupled with the effects of an 'anomalously' high pore water pressure.

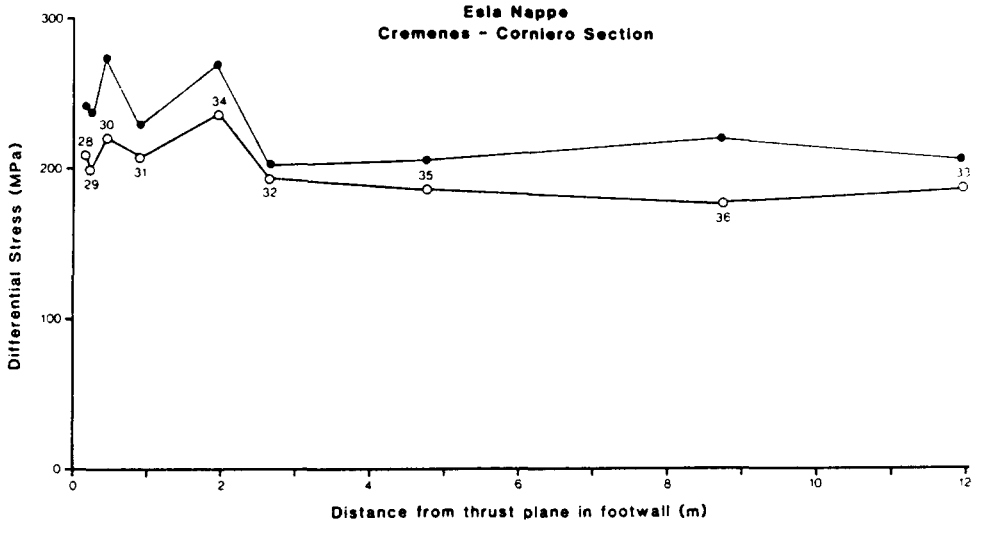

Fig. 15. Values of differential stress in the footwall of the Esla Nappe at different distances from the thrust plane, estimated by the V_{max} (open symbols) and twin density (closed symbols) methods. The twin density method estimates consistently higher stresses, but the form of variation of stress with distance from the thrust plane is the same in each case.

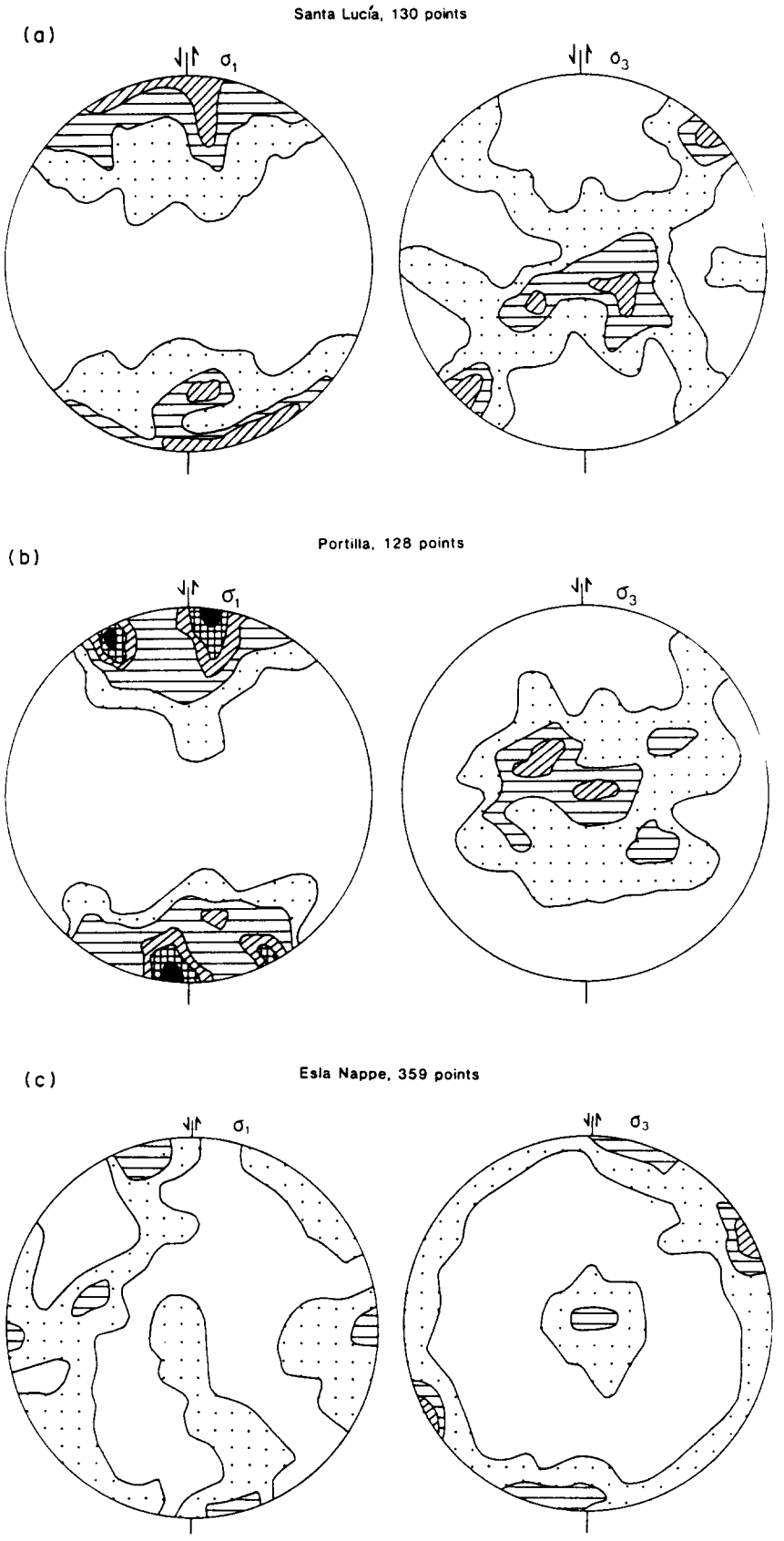

Fig. 16. Results of analyses of principal palaeostress orientations using the Turner Dynamic Analysis method, carried out on (the larger) grains containing at least 10 twin lamellae. The grains represented here are those which were most favourably oriented for twinning from at least three thin sections in each case. All data are shown relative to the thrust plane, oriented N–S and vertical, with the sense of shear as indicated. In the case of the Santa Lucía (specimens S.31.3 and S.31.6) and Portilla (specimens P.36.3 and P.36.5) localities, no significant difference was observed between the sections examined from above and below the thrust planes, therefore these data have been combined together in the contoured lower-hemisphere, equal-area projections shown here. All of the samples from the Esla Nappe locality were taken from the footwall, and data from four specimens (E.7.28, 30, 32 and 33) have been combined together in the diagrams shown. In all cases the lowest contour is 1 × uniform, increasing by 1 × uniform intervals through the shaded regions. By contouring in mutiples of a uniform distribution, comparisons can be made between diagrams prepared from different sample sizes.

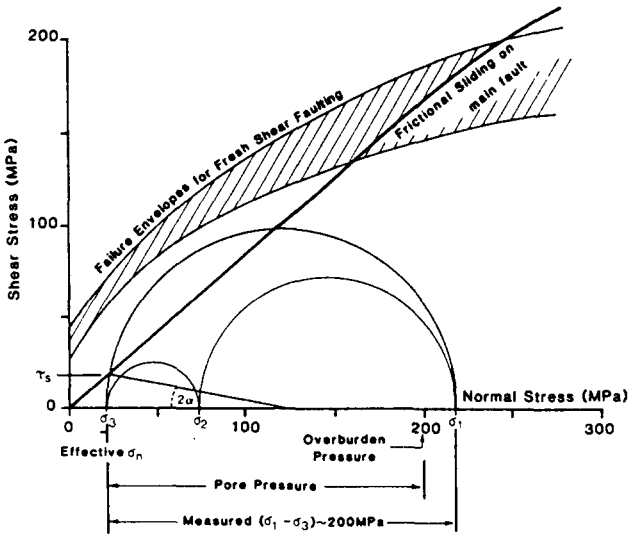

Fig. 17. Mohr diagram to illustrate conditions required for compatibility between a small resolved shear stress, τ_s, driving fault displacement and a large value (200 MPa) of differential stress, such that failure on sets of small faults, oblique to the main fault, does not occur. σ_1 and σ_3 would then lie near-parallel to the transport direction (minimum angle α) and normal to the fault plane, respectively. The pore fluid pressure must be about nine-tenths of the overburden pressure. The intact-rock failure envelopes, falling in the shaded area, and the small-displacement frictional sliding line are for limestones petrographically similar to those of the Cantabrian zone.

The occurrence of σ_3 lying in the fault plane (as observed from the Santa Lucía and Portilla localities) does not appear to be compatible with simultaneous fault slippage (driven by the stress difference $\sigma_1 - \sigma_2$) and a low resolved shear stress. However, it is possible that these stress conditions were attained prior to the development of the thrust surfaces, and do not relate to the thrust slippage part of the history at all. Alternatively, small displacement frictional strength data obtained in the laboratory may overestimate the long-term, large displacement frictional strength of calcite rocks in nature.

It is, however, unlikely that pore water pressure was normally high enough to make the least principal stress effectively zero. The uniaxial compressive strength of limestones like these is typically between 100 and 200 MPa (e.g. Rutter 1972), commensurate with or slightly lower than the $\sigma_1 - \sigma_3$ values estimated in this study.

In order to sustain such stress levels without the widespread development of small faults oriented obliquely to the main thrust planes, a small but significant effective confining pressure, perhaps up to a few tens of MPa, must normally have been present. These principles are illustrated graphically in Fig. 17.

The concentration of σ_3 axes in the fault planes is not optimal for fault slippage, for the shear stress resolved along the fault in the transport direction would be derived from $\sigma_1 - \sigma_2$, which must be less than the measured maximum stress difference, $\sigma_1 - \sigma_3$. Given the constraints mentioned above it appears unlikely that conditions for fault slippage could arise for small angles between σ_1 and the fault plane (see Fig. 17).

Remembering that these palaeopiezometric techniques record the *peak* stresses attained during the entire history of the rock mass, it is possible that the differential stress levels and principal stress orientations recorded do not relate to the period of thrust fault motion. They may have developed earlier, during the period of layer-parallel compression and bed flexure which must have preceded localization of the deformation onto the thrust plane, and represent the initial resistance of the rock pile to yield. Concentration of σ_3 axes in the plane of bedding and normal to the transport direction implies stretching of the layers in this direction. This may be brought about by local drape folding over a low amplitude lateral structure or through lateral variations in the amount of within-layer displacement in the transport direction. The similarity of stress orientations in both hanging and footwalls is also consistent with their development prior to fault localization. Sliding along a weak layer would be expected to result in σ_1 parallel to the transport direction in the hangingwall and σ_3 parallel to this direction in the footwall.

Clearly, the magnitude of the maximum recorded differential stress cannot be related simply to the average level of shear stress active along fault planes. From calcite twinning it is possible to obtain information regarding both the magnitude and orientation of palaeostresses. Other palaeopiezometers, such as dynamically recrystallized grain size in quartz, do not yield orientation information, therefore stress magnitudes obtained by such methods may not always be interpretable in terms of the shear stress levels resolved along a plastic fault zone.

The attainment of higher peak stresses and the wider spread of principal stress axes recorded from the Esla Nappe must be a consequence of a much greater amount of displacement on the thrust plane, about 1000 times greater than the displacements on the Santa Lucía and Portilla tectonic wedges. The weak concentrations of both σ_1 and σ_3 axes into a great circle girdle normal to the thrust plane and their intersection in the transport direction may have arisen by repeated flexure of the layers, first one way and then the other, as they were translated over the ramp-flat geometry of the underlying Corniero Thrust. Within the nappe pile (of which the Esla Nappe is the uppermost), there are also many lateral steps and folds. Draping of the layers around these is probably responsible for the wide spread of principal stress orientations recorded, and hence for the activation of twinning in every grain. Even if the frictional resistance to fault slippage was low, perhaps owing to high pore pressure or to an intrinsically low shear strength of the fault zone, the flexural resistance of the layers, requiring a large stress difference to overcome it, may have represented the principal barrier to nappe emplacement.

Two additional factors may contribute to the spreading of the principal stress axes around the great circle normal to the thrust plane:

(a) as the rocks are displaced past the ramps (or any other barrier to slip) the shear stress resolved along the fault locally increases, causing the principal stress axes to rotate temporarily away from the fault plane;

(b) the propagation of any kind of slip rate discontinuity (dislocation) along the fault, perhaps in response to hydrothermal cementation of the fault plane during a static period or during fault initiation, will cause a swing

in the orientation of the principal stresses and a large variation in their magnitude, according to the form of the stress field around the tip of a shear mode crack.

SUMMARY AND CONCLUSIONS

By means of high-temperature deformation experiments on calcite rocks of different grain sizes, we have established empirical relationships between differential stress and twinning incidence, twin density and volume fraction, and the way that these relationships depend on grain size. Both twinning incidence and volume fraction increase with grain size at a constant level of differential stress, but twin density is independent of grain size. At a given grain size, volume % twinning and I_t increase with differential stress. Twin density increases with stress and is independent of grain size. All of these measures of twinning activity are, within experimental uncertainty, independent of temperature, strain and strain rate.

Standard error values on stress determinations by the V_{max} and twin density methods are approximately 40 and 43 MPa, respectively, at any stress level. These figures are disappointingly large, but from further experimental studies it may prove possible to reduce them. Using the I_t method the standard error is smaller (30 MPa at any stress level), but the method can only be applied when the stress history has been simple. This can be assessed from the results of a Turner Dynamic Analysis (TDA) of the principal palaeostress orientations.

We have shown how these relationships can be used as a basis for the estimation of natural palaeostress magnitudes, and have illustrated this by means of a preliminary study of two areas of thrust faulting in the Cantabrian thrust belt of northern Spain. In both cases high peak differential stress levels were recorded (between 150 and 250 MPa). However, the TDA technique revealed the tendency of the maximum principal stress axes to be parallel to the fault surfaces, hence, at least in the case of faults of small displacement, the resolved shear stress along the fault slip vector must have been very low. The high differential stresses were inferred to have been induced mainly by flexure of the fault walls as they traversed irregularities during slip, coupled with high stresses induced prior to fault localization.

A more thorough understanding of natural distributions of palaeostress orientations and magnitudes will require a more detailed study of a large area in which the structural geometry can be well defined and the displacements are small.

Acknowledgements—Most of this work was carried out whilst K. J. Rowe was the holder of a N.E.R.C. research studentship. E. H. Rutter acknowledges a British Council travel grant under the Acciones Integradas program to support visits to Spain. Field studies in Spain were carried out with the permission of the Spanish National Commission for Geology. We are indebted to members of the geotectonics group at Oviedo University, Spain, for logistical support, discussions and for freely making available the pre-publication results of their new studies in the Cantabrian region. In particular, we thank Andrés Pérez-Estaun, Alberto Marcos, Juan-Luís Alonso, Florentino Díaz-García, Fernando Bastida, Javier Pulgar and Jorge Marquinez. We appreciate greatly the work of Robert Holloway in the Imperial College Rock Deformation Laboratory, who skilfully maintained the apparatus and assisted with the running of the experiments. C. J. Spiers provided a very helpful and constructive review of the manuscript.

REFERENCES

Alonso, J. L. 1987. Sequences of thrusts and displacement transfer in the superposed duplexes of the Esla Nappe Region (Cantabrian Zone, NW Spain). *J. Struct. Geol.* **9**, 969–983.

Carter, N. L. & Raleigh, C. B. 1969. Principal stress directions from plastic flow in crystals. *Bull. geol. Soc. Am.* **80**, 1231–1264.

Casey, M., Rutter, E. H., Schmid, S. M., Siddans, A. W. B. & Whalley, J. 1978. Texture development in experimentally deformed calcite rocks. *Proc. 5th Int. Conf. on Textures of Materials, Aachen* **2**, 231–240.

Friedman, M. 1964. Petrofabric techniques for the determination of principal stress directions in rocks. In: *State of Stress in the Earth's Crust* (edited by Judd, W. R.). Elsevier, New York, 451–550.

Friedman, M. & Conger, F. B. 1964. Dynamic interpretation of calcite twin lamellae in a naturally deformed fossil. *J. Geol.* **72**, 361–368.

Friedman, M. & Heard, H. C. 1974. Principal stress ratios in Cretaceous limestones from Texas Gulf Coast. *Bull. Am. Ass. Petrol. Geol.* **58**, 71–78.

Friedman, M. & Stearns, D. W. 1971. Relations between stresses inferred from calcite twin lamellae and macrofractures, Teton Anticline, Montana. *Bull. geol. Soc. Am.* **82**, 3151–3162.

Groshong, R. H. 1974. Experimental test of least-squares strain gage calculation using twinned calcite. *Bull. geol. Soc. Am.* **85**, 1855–1864.

Jamison, W. R. & Spang, J. H. 1976. Use of calcite twin lamellae to infer differential stress. *Bull. geol. Soc. Am.* **87**, 868–872.

Pérez-Estaun, A., Bastida, F., Alonso, J. L., Marquinez, J., Aller, J., Alvarez-Marrón, J., Marcos, A. & Pulgar, J. A. 1988. A thin-skinned tectonics model for an arcuate fold and thrust belt: the Cantabrian Zone (Variscan Ibero-Armorican Arc). *Tectonics* **7**, 517–538.

Rutter, E. H. 1972. The influence of interstitial water on the rheological behaviour of calcite rocks. *Tectonophysics* **14**, 13–33.

Rutter, E. H. 1974. The influence of temperature, strain-rate and interstitial water in the experimental deformation of calcite rocks. *Tectonophysics* **22**, 311–334.

Rutter, E. H., Peach, C. J., White, S. H. & Johnson, D. 1985. Experimental 'syntectonic' hydration of basalt. *J. Struct. Geol.* **7**, 251–266.

Schmid, S. M., Boland, J. N. & Paterson, M. S. 1977. Superplastic flow in finegrained limestone. *Tectonophysics* **43**, 357–391.

Schmid, S. M. & Paterson, M. S. 1977. Strain analysis in an experimentally deformed oolitic limestone. In: *Energetics of Geological Processes* (edited by Saxena, K. & Battacharji, S.). Springer-Verlag, New York, 67–93.

Schmid, S. M., Paterson, M. S. & Boland, J. N. 1980. High temperature flow and dynamic recrystallization in Carrara marble. *Tectonophysics* **65**, 245–280.

Spang, J. H. 1972. Numerical method for dynamic analysis of calcite twin lamellae. *Bull. geol. Soc. Am.* **83**, 467–472.

Spang, J. H. 1974. Numerical dynamic analysis of calcite twin lamellae in the Greenport Center syncline. *Am. J. Sci.* **274**, 1044–1058.

Spiers, C. J. 1979. Fabric development in polycrystals deformed at 400°C. *Bull. Minéral.* **102**, 282–289.

Spiers, C. J. 1982. The development of deformation textures in calcite rocks. Unpublished Ph.D thesis, University of London.

Spiers, C. J. & Rutter, E. H. 1984. A calcite twinning palaeopiezometer. In: *Progress in Experimental Petrology* (edited by Henderson, C. M. B.). *N.E.R.C. Publication Series* **D25**, 241–245.

Tullis, T. E. 1980. The use of mechanical twinning in minerals as a measure of shear stress magnitude. *J. geophys. Res.* **85**, 6263–6268.

Turner, F. J. 1953. Nature and dynamic interpretation of deformation in calcite of three marbles. *Am. J. Sci.* **251**, 276–298.

Turner, F. J. & Weiss, L. E. 1963. *Structural Analysis of Metamorphic Tectonites*. McGraw-Hill, New York.

White, S. H. 1979. Difficulties associated with palaeostress estimates. *Bull. Minéral.* **102**, 210–215.